Galactic Dynamics in the Era of Large Surveys
Proceedings IAU Symposium No. 353, 2019
M. Valluri & J. A. Sellwood, eds.

© International Astronomical Union 2020
doi:10.1017/S1743921319008524

Revisiting the innermost kinematics of M31 galaxy with the OMM Fabry-Perot interferometer

Sié Zacharie Kam[1], Claude Carignan[1,2,3], Michel Marcelin[4], Philippe Amram[3] and Jean Koulidiati[1]

[1]Laboratoire de Physique et de Chimie de l'Environnement, Université Joseph Ki-Zerbo, 03 BP 7021 Ouaga 03, Burkina Faso,
szachkam@gmail.com

[2]Department of Astronomy, University of Cape Town,Private Bag X3, Rondebosch 7701, South Africa,
ccarignan@astro.uct.ca

[3]Laboratoire d'Astrophysique Expérimentale (LAE), Département de physique, Université de Montréal, C.P. 6128, Succ. Centre-Ville, Montréal, QC, CanadaH3C 3J7

[4]Laboratoire d'Astrophysique de Marseille, Aix Marseille Univ, CNRS, Pôle de l'Étoile Site de Château-Gombert 38, rue Frédéric Joliot-Curie 13388 Marseille cedex 13 FRANCE

Abstract. We present observations on optical emission lines acquired with the scanning Fabry-Perot interferometer of the observatoire du Mont Mégantic, of the Andromeda galaxy (M31). A 765 order Fabry-Perot were used with a fast readout EM-CCD. From data obtained, kinematic maps and data points for the rotation curve of the innermost part of the galaxy are derived. Several dozen of regions have been scanned with the Fabry-Perot interferometer and narrow band interference filters. The central 10'x10' were scanned with five different filters. Observations have been made in order to get better Hα data for kinematics purposes.

Keywords. galaxies: individual (Andromeda), galaxies: kinematics and dynamics

1. M31 kinematics

The Andromeda galaxy, is the most massive galaxy nearby the Milky Way. The first part of Table 1 summarize its optical parameters. M31 (also called NGC0224) is well define in the infrared observations and appears as a disk with ring like structure (Devereux *et al.* 1994). A better understanding of M31 through photometry, dynamics and kinematics studies allows us to better know our own Galaxy. Observing the Andromeda galaxy neighbourhood, one detect different filamentary structure and its halo reveals past interactions with M33, M32 and NCG 205 (Thilker *et al.* (2004); Grossi *et al.* (2008); McConnachie *et al.* (2009)). M31 disk at large scale is warped (Newton & Emerson (1977); Braun (1991); Corbelli *et al.* (2010)) and the observation of HI lines present in most of case multiple emission peaks on HI lines Chemin *et al.* (2009).

As the massive galaxies, M31 has a massive black hole, (Kormendy *et al.* (1988), Gültekin *et al.* (2009)) and Menezes *et al.* (2012) fund an Hα emitting disk in the innermost part. Despite the detection of Hα emission around the central black hole, the star formation is low due to the low fraction of gas in the inner part (Melchior *et al.* 2017). Many studies on M31 kinematics have been done. Since Rubin *et al.* (1970)'s work on M31's rotation curve (RC) diverse observations and analysis have been done using different lines. The RC from Rubin *et al.* (1970), Newton & Emerson (1977), Braun (1991),

https://doi.org/10.1017/S1743921319008524 Published online by Cambridge University Press

Table 1. Parameters of M 31 and kinematical studies results.

Parameters	Value	Source
Morphological type	SA(s)cd	RC3
R.A. (2000)	$00^h42^m\ 44.4^s$	CSC
Dec. (2000)	$+41°\ 16'\ 08.6''$	CSC
Systemic Velocity (km.s^{-1})	-300 ± 3	RC3
Distance	780 kpc	
Scale (pc/arcmin)	3.8pc/′	
Inclination, i	$77° \pm 3°$	
PA (major axis)	$35° \pm 1°$	
Total HI mass ($M_\odot$)	$1.95 \pm 0.36 \times 10^9$	
Systemic Velocity (km.s^{-1})	-300 ± 3	Schechter & Gunn 1979
V_{rot} maximum (km.s^{-1})	253	
Stellar mass ($M_\odot$), w1	$6.3 \pm 0.3 \times 10^9$	
Virial mass ($M_\odot$) (at 159 kpc)	$\sim 1.1 \pm 0.6 \times 10^{12}$	Chemin *et al.* (2009)

RC3: de Vaucouleurs *et al.* 1991
SCS: The Chandra Source Catalog Evans *et al.* (2010)

Carignan *et al.* (2006) and Chemin *et al.* 2009 show the higher velocity pics at the inner part of the galaxy. The RC seems more stable at 230 ± 4 km.s^{-1}around $95' < R < 120'$ Chemin *et al.* 2009. The better mass models for M31 are obtained using spheroidal bulge, stellar disk, usually exponential, interstellar gas and central black hole. Especially Chemin *et al.* 2009 considered the contribution of the molecular gas (H_2), derived form Dame *et al.* 1993 CO observations. Braun *et al.* (1991) found M31 dynamical mass to be $(2.0 \pm 0.1) \times 10^{11}$ $M_\odot$at $R < 28$ kpc since the observations of Chemin *et al.* 2009 found two times massive probing up to 38 kpc. For better modelling of galaxies, accurate constraints are needed, for that, deep surveys are essential to extract RC and kinematic parameters for mass model purposes. A good determination of the rising part of a rotation curve makes it possible to define the associated mass model. The observations of the innermost kilo parsecs of the galaxy therefore require a good resolution.

This paper presents the Hα observation for a kinematics analysis of M31 innermost part, it is dedicated on deriving the optical rotation curve and extracting the kinematical parameters from Hα Fabry-Perot observations.

2. Observation and data reduction

Between September 2012 to December 2016, M31 was observed at Observatoire du Mont Mégantic (OMM) in Canada. The 1.6 m telescope of OMM has been for the M31 Hα and NII survey. A 765 order Fabry-Perrot and Andor EMCC camera (IXON888) was also used for data acquisition. The central part is observed with four different filters : filter Hα-300 centered at $\lambda_c = 6560$ Å, filter M1 centered at $\lambda_c = 6557$ Å; filter M3 centered at $\lambda_c = 6585$ Å; filter #76 centered at $\lambda_c = 6567.7$ Åand the #78 centered at $\lambda_c = 6587.7$ Å. The FP is scanned through forty-height (48) channels to produce the Raw data. The useful data cube is wavelength-sorted with a correction of the airmass variation during the long time of acquisition. The reduction process takes into account the correction of the guiding shift. The following steps were adopted for the reduction of data:

(a) Correction of all data with the normalized flat image.
(b) Creation of a wavelength-sorted data cube corrected, cosmic rays, noise.
(c) Ghosts correction (see Epinat *et al.* 2008).
(d) Heliocentric velocity correction, including a correction for the induced initial shift.
(e) Hanning spectral smoothing and sky subtraction (eg. Daigle *et al.* 2006).
(f) Single line fitting procedure.
(g) Extraction of the velocity, dispersion and Hα integrated maps.

https://doi.org/10.1017/S1743921319008524 Published online by Cambridge University Press

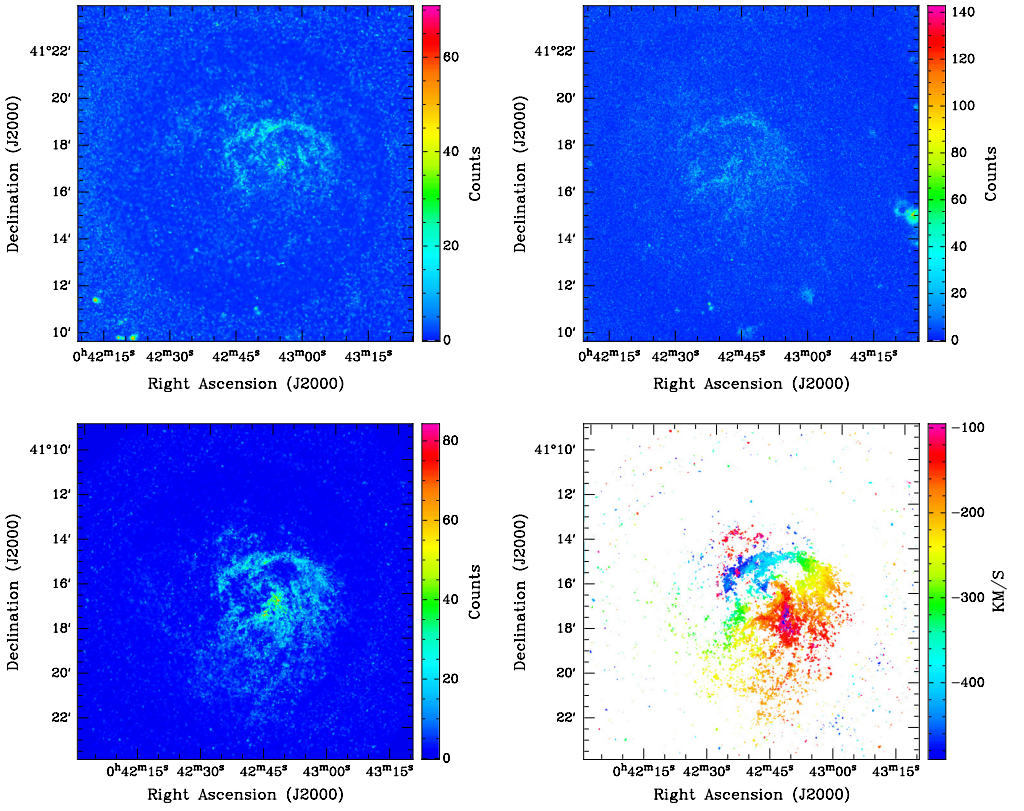

Figure 1. Innermost 10 arcmin : the top left image give the Hα emission with the filter Hα -300 and at top right image the Hα emission withe the filter M1. The bottom left image is the NII emission map and the bottom right image is the optical velocity map given by M3 filter.

3. Preliminary Results

Different filters have been used to highlight the center of M31. For the preliminary results allows us to define the NII and the Hα clearly in the central part. The sample of the data presented in figure 1 show the weakness of the Hα compared to the NII in Andromeda galaxy.

The cut-off wavelength of the Hα-300 filter shows that it is the best filter for observing the central region of M31. The low transmission ($\sim$40 %) of the Hα-300 filter remains a handicap in its use. Therefore takes a very long time to get usable results. The Filter M1 is less narrow but with a good inclination, it permits to make good observations of M31. The result of the observations gives a good concordance with the emissions observed by Ciardullo *et al.* (1988).

A total of more than fifteen (15) data cubes and more than twenty-two hours of observation of the central part of M31 have been done. The finesse is a quantity which relates the free spectral range (FSR) to the full-width half-maximum, $\delta\lambda$, of a transmission band. The finesse can be approximated by $f = \frac{\pi\ R^{\frac{1}{2}}}{1-R}$, where R is the reflectance of the Fabry-Perot surfaces. More the value of the finesse is great, better are the details of the observed field. For our observation the minimum finesse use for our observations is $f = 16$, this enables a resolution about 12000 at Hα. As shown in the figure 1, the observations give the velocity maps. The dispersion maps can be also derived during the process. The central field alone cannot give a good approximation of the mass of galaxy M31. We added some points obtained by our observations to the data of Chemin *et al.* (2009) and the

https://doi.org/10.1017/S1743921319008524 Published online by Cambridge University Press

second part of Table 1 gives us values quite similar to their results. This was predictable, seeing the low weight that our data represents (∼11' vs 150'). The complement of the other fields observed will give a good orientation of the mass model.

This new mapping will allow us to calculate more accurate kinematical parameters of M31 by combining the HI already well known with the high-resolution data in the optical. Despite the high resolution of the 765 order FP and a long exposure time for our observations, the emission of warm gas Hα is weaker than NII and not symmetrical around the center. This preliminary result shows the possibility to add data points to the innermost part of the rotation curve via the Hα and NII observations of M31. This would helps to determine the best mass model of the Andromeda galaxy.

References

Block, D. L. *et al.* 2006, *Nature* 443, 832
Braun, R. 1991, *ApJ*, 372, 54
Carignan, C., Chemin, L., Huchtmeier, W. K., & Lockman, F. J. 2006, *ApJ*, 641, L109
Chemin, L., Carignan, C., & Foster, T. 2009, *ApJ*, 705, 1395
Ciardullo, R., Rubin, V. C., Ford, Jr., W. K., Jacoby, G. H., & Ford, H. C. E. 1988, *AJ*, 95, 438–444
Corbelli, E., Lorenzoni, S., Walterbos, R., Braun, R., & Thilker, D. 2010, *A&A*, 511, A89
Daigle, O., Carignan, C., Hernandez, O., Chemin, L., & Amram, P. 2006, *MNRAS*, 368, 1016
Daigle, O., Gach, J., Guillaume, C., Lessard, S., Carignan, C., & Blais-Ouellette, S. 2008, *in Society of Photo-Optical Instrumentation Engineers (SPIE) Conference Series*. p. 70146L
Dame, T. M., Koper, E., Israel, F. P., & Thaddeus, P. 1993, *ApJ*, 418, 730
Devereux, N., Price, R., Wells, L. A., & Duric, N. 1994, *AJ*, 108, 1667
Epinat, B. *et al.* 2008, *MNRAS*, 388, 500
Evans, I. N. *et al.* 2010, *ApJ Supplement Series*, 189, 37
Grossi, M., Giovanardi, C., Corbelli, E., Giovanelli, R., Haynes, M. P., Martin, A. M., Saintonge, A., & Dowell, J. D. 2008, *A&A*, 487, 161
Gültekin, K. *et al.* 2009, *ApJ*, 698, 198
Jarrett, T. H., Chester, T., Cutri, R., Schneider, S. E., & Huchra, J. P. 2003, *AJ*, 125, 525
Kam, Z. S., Carignan, C., Chemin, L., Amram, P., & Epinat, B. 2015, *MNRAS*, 449, 4048
Kormendy, J. 1988, *ApJ*, 325, 128
McConnachie, A. W. *et al.* 2009, *Nature*, 461, 66
Melchior, A.-L. & Combes, F. 2017, *A&A* , 607, L7
Menezes, R. B., Steiner, J. E., & Ricci, T. V. 2012, *ApJ*, 762, L29
Newton, K. & Emerson, D. 1977, *MNRAS*, 181, 573
Rubin, V. C. & Ford W. Kent, J. 1970, *ApJ*, 159, 379
Schechter, P. L. & Gunn, J. E. 1979, *AJ*, 229, 472
Thilker, D. A., Braun, R., Walterbos, R. A. M., Corbelli, E., Lockman, F. J., Murphy, E., & Maddalena, R. 2004, *ApJL*, 601, L39
de Vaucouleurs, G., de Vaucouleurs, A., Corwin, Jr. H. G., Buta, R. J., Paturel, G., & Fouque, P. 1991, *Sky & Telesc*, 82, 621

https://doi.org/10.1017/S1743921319008524 Published online by Cambridge University Press